

RESEARCH

Open Access



Cholesterol promotes EGFR-TKIs resistance in NSCLC by inducing EGFR/Src/Erk/SP1 signaling-mediated ERR α re-expression

Zhenzhen Pan^{1†}, Kai Wang^{1†}, Xiniao Wang^{1†}, Zhirong Jia¹, Yuqi Yang², Yalei Duan¹, Lianzhan Huang¹, Zhuo-Xun Wu², Jian-ye Zhang^{3*} and Xuansheng Ding^{1*}

Abstract

Background: The use of epidermal growth factor receptor tyrosine kinase inhibitors (EGFR-TKIs) brings remarkable benefits for the survival of patients with advanced NSCLC harboring EGFR mutations. Unfortunately, acquired resistance seems to be inevitable and limits the application of EGFR-TKIs in clinical practice. This study reported a common molecular mechanism sustaining resistance and potential treatment options to overcome EGFR-TKIs resistance.

Methods: EGFR-TKIs resistant NSCLC cells were established and confirmed by MTT assay. Cholesterol content was detected and the promotional function of cholesterol on NSCLC growth was determined in vivo. Then, we identified ERR α expression as the downstream factor of cholesterol-mediated drug resistance. To dissect the regulatory mechanism, we conducted experiments, including immunofluorescence, co-immunoprecipitation, luciferase reporter assay and chromatin immunoprecipitation assay.

Results: Long-term exposure to EGFR-TKIs generate drug resistance with the characteristic of cholesterol accumulation in lipid rafts, which promotes EGFR and Src to interact and lead EGFR/Src/Erk signaling reactivation-mediated SP1 nuclear translocation and ERR α re-expression. Further investigation identifies ERR α as a target gene of SP1. Functionally, re-expression of ERR α sustains cell proliferation by regulating ROS detoxification process. Lovastatin, a drug used to decrease cholesterol level, and XCT790, an inverse agonist of ERR α , overcome gefitinib and osimertinib resistance both in vitro and in vivo.

Conclusions: Our study indicates that cholesterol/EGFR/Src/Erk/SP1 axis-induced ERR α re-expression promotes survival of gefitinib and osimertinib-resistant cancer cells. Besides, we demonstrate the potential of lowering cholesterol and downregulation of ERR α as effective adjuvant treatment of NSCLC.

Keywords: Non-small cell lung cancer, EGFR-TKIs resistance, Cholesterol

Background

Epidermal growth factor receptor (EGFR) is reported as an important driver oncogene in non-small cell lung cancer (NSCLC) [1]. Patients harboring EGFR mutations, including the exon 19 deletion and L858R point mutation, initially respond well to EGFR tyrosine kinase inhibitors (EGFR-TKIs) [2, 3]. However, most patients will eventually develop acquired resistance after 9-12 months of treatment [4, 5]. The most

*Correspondence: jjanyez@163.com; 1020030749@cpu.edu.cn

[†]Zhenzhen Pan, Kai Wang and Xiniao Wang contributed equally to this work.

¹ School of Basic Medicine and Clinical Pharmacy, China Pharmaceutical University, Nanjing 211198, Jiangsu, China

³ Key Laboratory of Molecular Target & Clinical Pharmacology and the State & NMPA Key Laboratory of Respiratory Disease, School of Pharmaceutical Sciences & The Fifth Affiliated Hospital, Guangzhou Medical University, Guangzhou 511436, China

Full list of author information is available at the end of the article



common mechanism of resistance in patients using either the first- or the second-generation EGFR-TKIs is second-site mutation T790M of EGFR exon 20 [6]. The third-generation EGFR-TKIs, including osimertinib and olmutinib, are developed to overcome T790M mutation-mediated resistance [7, 8]. Based on clinical trials, osimertinib become the standard second-line treatment in NSCLC patients harboring T790M mutation [9]. In recent years, osimertinib shows superior overall survival (OS) and progression free survival (PFS) compared with the first-generation EGFR-TKIs (gefitinib or erlotinib) as first-line treatment in NSCLC patients with EGFR mutations [10]. Although osimertinib exhibits promising clinical results, acquired resistance inevitably develops with a median PFS of 19 months in the first-line and 11 months in the second-line treatment [11]. Development of resistance to either the first- or the third-generation EGFR-TKIs limits their therapeutic efficacy. Thus, it is important to identify the drug resistance mechanisms to guide therapeutic regimen.

Reprogramming of lipid metabolism is a hallmark of cancers [12, 13]. As a crucial component of lipids, cholesterol is recognized to be essential for cancer cell proliferation and survival [14]. Apart from being a constituent of cell membrane, cholesterol is widely distributed in lipid rafts, small domains within the cell membrane that represent as platforms involved in cellular signaling transduction [15]. Mammalian cells maintain cholesterol homeostasis through regulation of de novo synthesis, uptake, efflux and storage progress [16]. Most recently, content of cholesterol is found to be upregulated in NSCLC cells or tumor xenograft models that resistant to the first-generation EGFR-TKIs as the result of increased biosynthesis, uptake and reduced efflux. Accumulation of cholesterol is regarded as an important factor of resistance to the first-generation EGFR-TKIs [17–19]. However, the mechanisms of cholesterol confer resistance to EGFR-TKIs are not well-revealed.

Estrogen related receptor alpha (ERR α) belongs to the orphan nuclear receptor superfamily and is encoded by the ESRRA gene. As a transcription factor, ERR α is well-known to regulate mitochondrial and metabolic genes involved in cellular energy metabolism [20]. Besides normal metabolism, ERR α exhibits oncogenic functions in various human cancers including lung cancer, breast cancer, prostate cancer and colon cancer [21–23]. The expression of ERR α is upregulated in lung cancer and its overexpression is related to poor survival in patients, suggesting that ERR α can be a druggable target for cancer therapy [24–26]. Moreover, accumulating evidence indicates that intracellular cholesterol is closely linked to the expression and activation of ERR α in breast cancer

[27–29]. However, little is known regarding the relationship between cholesterol and ERR α in NSCLC.

In the present study, we investigate cholesterol level in NSCLC and observe that accumulation of cholesterol in lipid rafts correlate to the resistance to both the first- and the third-generation EGFR-TKIs. We identify a regulatory role of cholesterol in ERR α re-expression and elucidate the underlying mechanisms. Mechanistically, we uncover that accumulation of cholesterol in lipid rafts reactivates EGFR/Src/Erk signaling pathway and promotes SP1 nuclear translocation, which enables ERR α transcription in the presence of EGFR-TKIs that is critical to NSCLC resistance.

Methods

Reagents

Gefitinib and lovastatin were purchased from Aladdin (Shanghai, China). Osimertinib was obtained from Glpbio (Montclair, CA, USA). XCT790, BAY 11-7082, WH-4-023 and Plicamycin were purchased from MCE (New Jersey, USA). Rapamycin, Y27632 and SCH772984 were obtained from AbMole (Houston, TX, USA). Lapatinib, AG-490 and mevalonate were obtained from Topscience (Shanghai, China). SIS3 was purchased from Selleck (Shanghai, China). Cholesterol and M β CD were obtained from Sigma-Aldrich (St Louis, MO, USA).

Cell culture

For all experiments, human NSCLC cell line PC-9 (BCRJ, Rio de Janeiro, Brazil), PC-9/GR, H1975 (Cell Bank of the Shanghai Academy of Life Sciences, Shanghai, China), and PC-9/OR were maintained in Dulbecco modified Eagle medium (KGM12800N-500, KeyGen BioTech, Nanjing, China) supplemented with 10% fetal bovine serum (086150, Wisent, St-Bruno, Quebec, Canada), 100 μ g/mL streptomycin and 100 U/mL penicillin (ST488, Beyotime Biotechnology, Shanghai, China) in a humidified cell culture incubator at 37 °C with an atmosphere of 5% CO₂.

Transfection

For cell transfection, 100 nM siEGFR (the target sequence: 5'-GCAACAUGUCGAUGGACUUTT-3') (HanBio, Shanghai, China) and 2.5 μ g pCDNA3.1 or pCDNA3.1-SP1 (Genomeditech, Shanghai, China) were transfected into NSCLC cells with Lipofectamine 2000 (11668-019, Invitrogen, Carlsbad, CA, USA) growing in serum-free opti-MEM media (51985-034, Gibco, Gaithersburg, MD, USA).

Western blot

For evaluating protein expression in cells or tumor tissues, proteins were extracted. The same amounts of

proteins were separated through 10-15% SDS-PAGE and transferred to polyvinylidene difluoride membranes, following by blocking with 5% nonfat milk. Subsequently, the membranes were incubated with primary antibodies, then with secondary antibodies. Immunoblot signals were visualized by ECL detection and the expression of proteins was quantified by Image J software. Antibodies used for Western blot were: anti-p-EGFR, anti-EGFR, anti-Erk, anti-SP1 (Cell Signaling Technology, Boston, MA, USA); anti-GAPDH, anti-p-Erk (Proteintech, Wuhan, China); anti-p-Src (Affinity Biosciences, Changzhou, China); anti-Lamin B (Wanleibio, Shenyang, China); anti-Caveolin1 (HUABIO, Hangzhou, China); anti-ERR α , anti-Src, HRP-labeled goat anti-rabbit IgG(H+L) (Beyotime Biotechnology, Shanghai, China).

RT-qPCR

Trizol reagent (R401-01, Vazyme, Nanjing, China) was used to extract total RNAs from NSCLC cells as described by the manufacturer's instructions. cDNA was synthesized using mRNA as a template with HiScript III RT SuperMix (R323-01, Vazyme, Nanjing, China). ChamQ SYBR qPCR Master Mix (Q341-02, Vazyme, Nanjing, China) was used for RT-qPCR analysis. GAPDH expression was used to normalize the data. The mRNA primer sequences used are shown as below: 5'-GTCTCC TCTGACTTCAACAGCG-3' and 5'-ACCACCCTGTTG CTGTAGCCAA-3' for GAPDH; 5'-CCTCTGTGACCT CTTTGACC-3' and 5'-TACTGACATCTGGTCAGAC-3' for ERR α [30].

Cell viability assay

Cell viability was determined by MTT assay. Cells were treated with indicated drugs following by adding 0.5 mg/mL MTT solution (3580GR001, Biofrox, Guangzhou, China) at 37°C for 4 h. Finally, the absorbance of each well was measured using a microplate reader.

Luciferase reporter assay

Cells were transfected with pRL-TK and pGMERR α -Lu (Genomeditech, Shanghai, China) and cultured in medium with indicated drugs for 36 h. Subsequently, cells were lysed with 1 \times cell lysis buffer at room temperature for 5 min and the luciferase activities were detected with Dual-Luciferase Reporter Assay System (DL101-01, Vazyme, Nanjing, China). Renilla luciferase activity was used to normalize the firefly luciferase activity.

Co-immunoprecipitation (co-IP)

Cells were treated with indicated drugs and collected, then lysed in RIPA lysis buffer (KGP703-100, Key-Gen BioTech, Nanjing, China). Lysates were centrifuged at 14,000g, 4°C for 10 min and supernatant were

transferred to another tube with EGFR primary antibody (1:100, 4267S, Cell Signaling Technology, Boston, MA, USA) incubated overnight at 4°C. Then, the protein complexes were collected by incubation with 60 μ L of Protein A + G Agarose (P2055, Beyotime Biotechnology, Shanghai, China) for 1 h. Finally, the protein complexes were washed with RIPA lysis buffer and analyzed by Western blot assay.

CHIP assay

Chromatin immunoprecipitation (CHIP) assay was conducted following the manufacturer's instructions of the CHIP assay kit (P2078, Beyotime Biotechnology, Shanghai, China). Briefly, H1975 cells were fixed with 1% formaldehyde for 10 min, quenched in glycine for 5 min, washed and lysed in SDS lysis buffer. Cell lysates were sonicated until the DNA fragments were 200-1000 bp in size. Then the lysates were collected and pre-cleared with Protein A + G Agarose/Salmon Sperm DNA for 30 min. 2% percent of the chromatin was used as input control and the rest was incubated with antibody against IgG (1:100, A7016, Beyotime Biotechnology, Shanghai, China) and SP1 (1:100, 9389S, Cell Signaling Technology, Boston, MA, USA) overnight at 4°C. The chromatin complexes were then incubated with Protein A + G Agarose/Salmon Sperm DNA for 1 h at 4°C, following by washed with low salt immune complex wash buffer, high salt immune complex wash buffer, LiCl immune complex wash buffer, TE buffer and elution buffer (1% SDS, 0.1 M NaHCO₃). The DNA-protein complexes were incubated with 0.2 M NaCl overnight at 65°C, RNase A for 30 min at 37°C, proteinase K (ST532, Beyotime Biotechnology, Shanghai, China) for 1.5 h at 45°C. The DNA was purified using a DNA Clean Up Kit (D0033, Beyotime Biotechnology, Shanghai, China). Finally, the precipitated DNA was quantified using qPCR. Primers used for ERR α were: 5'-TGACCCCATCCGAGTGGAAATTTGAGT-3' and 5'-AGAAAGCTCAAGGTCACCTGCGGTG for-3'.

Immunofluorescence

For EGFR and Src fluorescence colocalization analysis, cells were seeded and exposed to the indicated drugs. Then, cells were fixed with 4% paraformaldehyde, blocked with goat serum and incubated with primary antibody against EGFR (1:100, 4267S, Cell Signaling Technology, Boston, MA, USA) overnight at 4°C. CoraLite[®]594-conjugated c-SRC (1:100, CL594-60315, Proteintech, Wuhan, China) and Goat Anti-Rabbit IgG H&L (FITC) (1:100, ab97050, Abcam, Cambridge, MA, USA) were used to treated the cells for 2 h at 37°C. nucleus was counterstained with 5 μ g/mL DAPI (C1002, Beyotime Biotechnology, Shanghai, China) for 10 min at room temperature. All images were taken with Zeiss LSM800 and

measured by Image Pro Plus software [31]. Pearson's correlation coefficient was calculated by Image J software [32, 33].

IHC

One-Step IHC Assay kit (KGOS60, KeyGen BioTech, Nanjing, China) was used for immunohistochemical (IHC) staining. Tissue slides acquired from NSCLC xenografts were deparaffinized and rehydrated, following by antigen retrieval, permeabilized and 3% H₂O₂ treatment. After being blocked with goat serum, slides were incubated with primary antibody against Ki67 (1:100, WL01384a, Wanleibio, Shenyang, China) or ERR α (1:100, sc-65715, Santa Cruz Biotechnology, Dallas, TX, USA) overnight at 4°C. On the second day, immune complexes were determined with horseradish peroxidase conjugates using DAB detection.

Nuclear protein extraction

The nuclear protein was extracted using Nuclear and Cytoplasmic Protein Extraction Kit (P0027, Beyotime Biotechnology, Shanghai, China) according to the manufacturer's instructions. Briefly, cells that have been treated with indicated drugs were harvested and dissociated in 200 μ L Reagent A mixture containing 1 mM PMSF (KGP610, KeyGen BioTech, Nanjing, China). The cell suspension was incubated on ice for 15 min. Then, 10 μ L Reagent B was added and the mixture was vortexed for 5 s with 1 min ice bath, following by centrifugation at 16,000 g, 4°C for 5 min. The supernatant was collected as cytoplasmic protein and the precipitation was further resuspended in 50 μ L nuclear protein extraction reagent containing 1 mM PMSF. After being vortexed and ice bath in turn for 30 min, the mixture was centrifuged at 16,000 g, 4°C for 5 min and the supernatant was saved as nuclear protein. The subcellular fractions were analyzed by Western blot assay.

Isolation of lipid rafts [34]

Cells were seeded, treated with indicated drugs and collected. The lysis buffer (20 mM Tris-HCl (pH 7.5),

150 mM NaCl, 0.5% Triton X-100) was used to lyse cells for 30 min. Then, the lysates were centrifuged at 16,000 g, 4°C for 30 min and supernatants were collected and referred to as the non-lipid rafts fractions. The rest insoluble pellets were added with 200 μ L buffer (0.5% SDS and 2 mM DTT), re-suspended and incubated for 10 min. Finally, the samples were centrifuged at 16,000 g, 4°C for 30 min and the supernatants were collected into another tubes, referring to as lipid rafts fractions.

Tumor xenograft model

BALB/c nude mice (4 weeks old) (Yangzhou University, Yangzhou, China) were housed under individual ventilated cages in compliance with the institutional guidelines. Mice were randomly assigned into four groups ($n = 5$), injected with PC-9, PC-9/GR, H1975 and PC-9/OR cells subcutaneously. We monitored the tumor volume every 3 days. In the second xenograft experiments, PC-9/GR cells were subcutaneously injected into the mice. After 1 week injection, mice were randomly assigned into three groups ($n = 5$) according to tumor volume as follows: gefitinib group (treat with 50 mg/kg gefitinib), gefitinib + lovastatin group (treat with 50 mg/kg gefitinib and 100 mg/kg lovastatin), and gefitinib + XCT790 group (treat with 50 mg/kg gefitinib and 8 mg/kg XCT790). In all experiments, gefitinib and lovastatin were administrated by oral gavage daily, while XCT790 was administrated by intraperitoneal injection. The tumor volume was measured every 3 days and calculated based on the formula: tumor volume (mm^3) = (length \times width²)/2. After approximately 3 weeks, mice were sacrificed and xenografts tissue were collected for further analysis.

Statistical analysis

Data were presented as mean \pm SEM and statistical analysis were performed by GraphPad Prism 8.0 software (GraphPad Software Inc., CA, USA). Unpaired Student's t test was used to compare differences between two groups, while analysis of variance (ANOVA) was used for comparisons among multiple groups. The Kaplan–Meier method was used for survival analysis, and the log-rank test was used to

(See figure on next page.)

Fig. 1 Accumulation of cholesterol in lipid rafts is responsible for EGFR-TKIs resistance. **a, b** PC-9 cells were exposed to gefitinib or osimertinib for 12 weeks to establish the gefitinib-resistant PC-9/GR and osimertinib-resistant PC-9/OR cells. **c, d** MTT assay was conducted to detect cell viability of NSCLC cells treated with gefitinib or osimertinib. **e, f** An Amplex[®] Red Cholesterol Assay Kit (A12216, Invitrogen, Carlsbad, CA, USA) was used to determine cholesterol level in the cytoplasm or lipid rafts of NSCLC cells. **g** Cells were incubated with 0.5 mg/mL Filipin (MB1848, Meilunbio, Dalian, China) for 2 h. Confocal images showed the free cholesterol in blue and the fluorescence intensity was analyzed. **h-m** Primary tumor gross appearance, **i** growth curves, **j** body weight, and **k** tumor weight of the tumor xenograft. **l** Cholesterol level in tumor tissues was determined. **m** IHC staining detected Ki67 expression in the indicated tumors. Data are expressed as mean \pm SEM ($n = 3$) * $p < 0.05$, ** $p < 0.01$, *** $p < 0.001$ in **c, d, e, f, g** and **l**. Data are expressed as mean \pm SEM ($n = 5$) * $p < 0.05$, ** $p < 0.01$, *** $p < 0.001$ in **k**

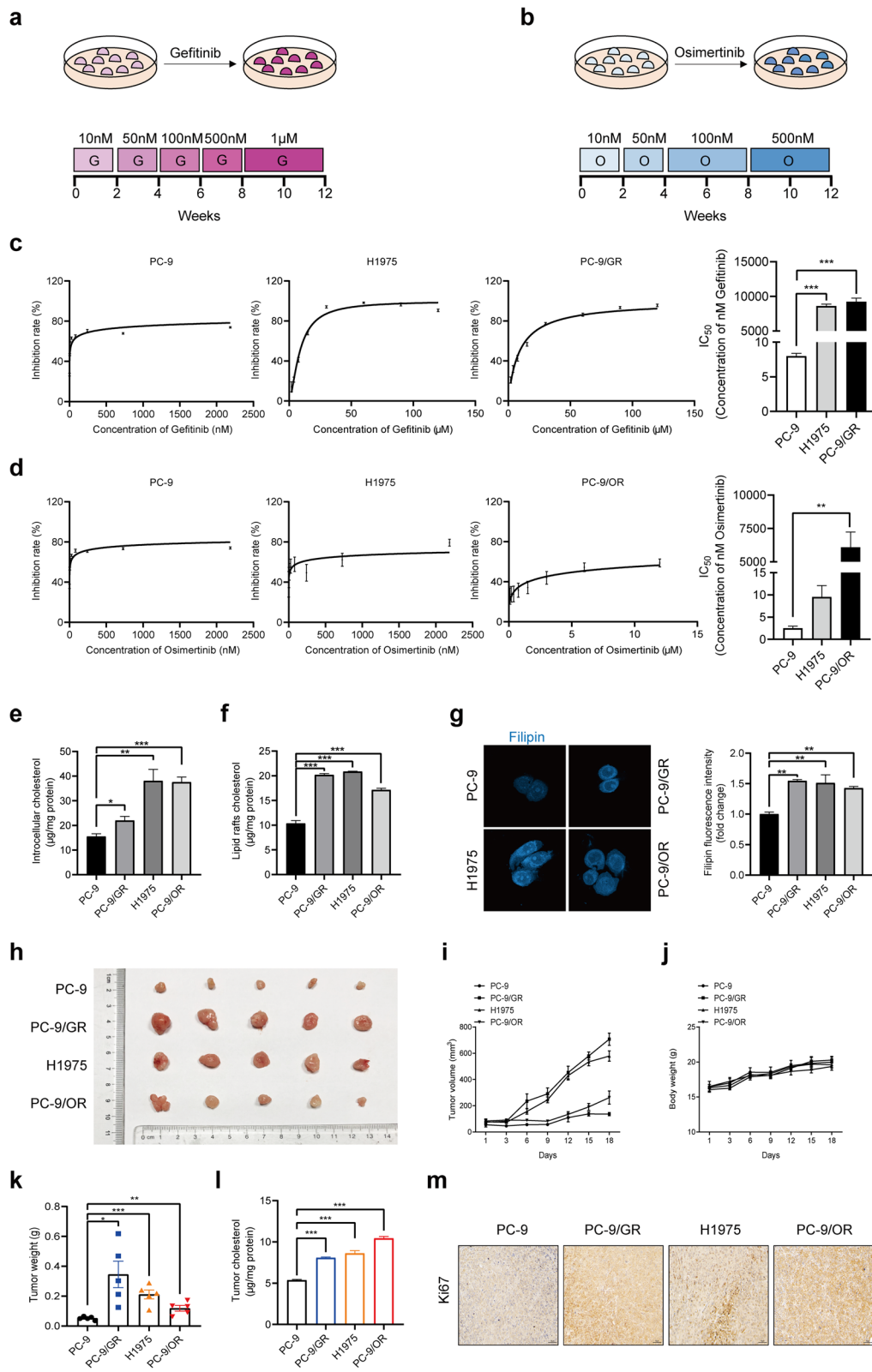


Fig. 1 (See legend on previous page.)

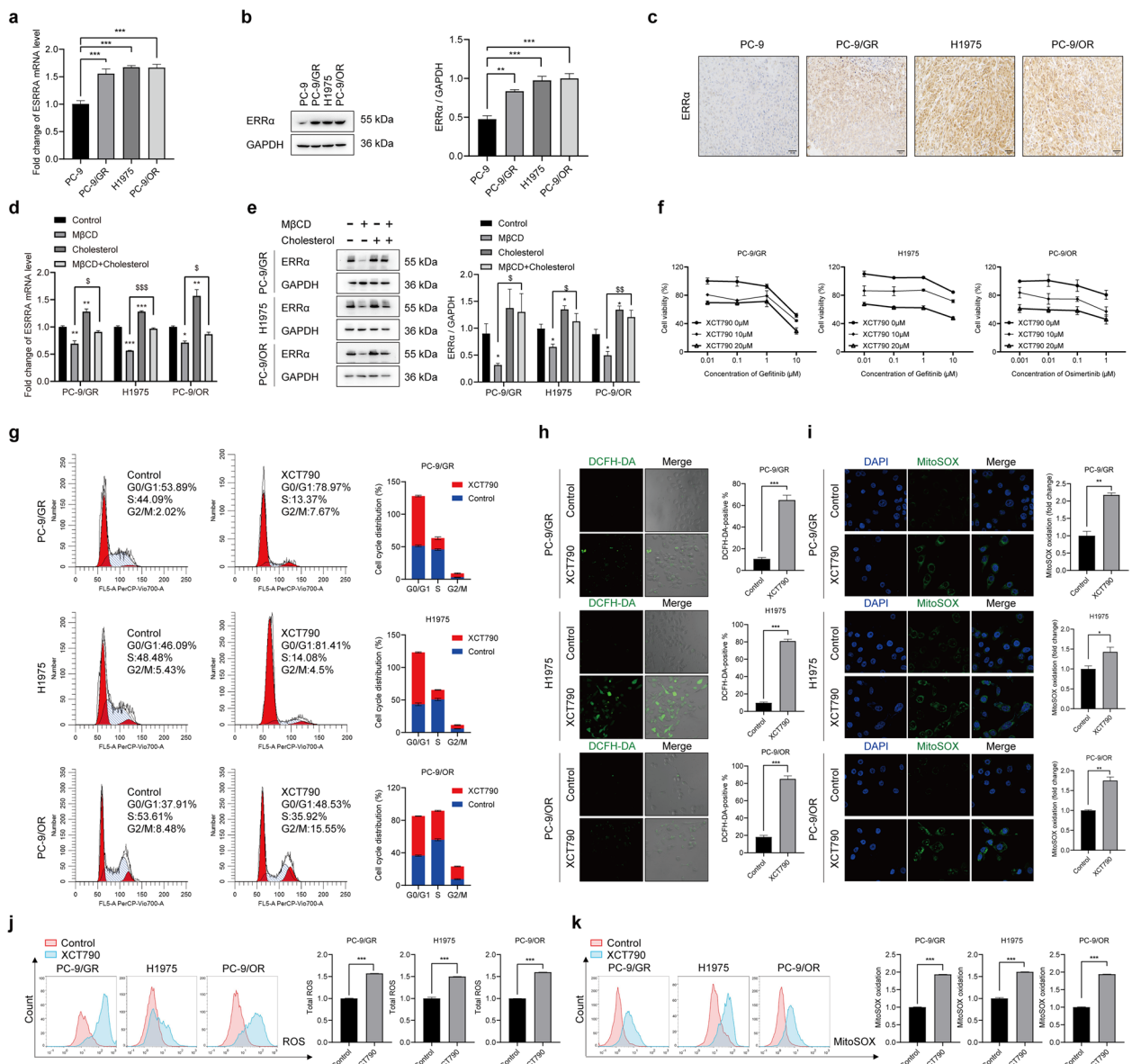
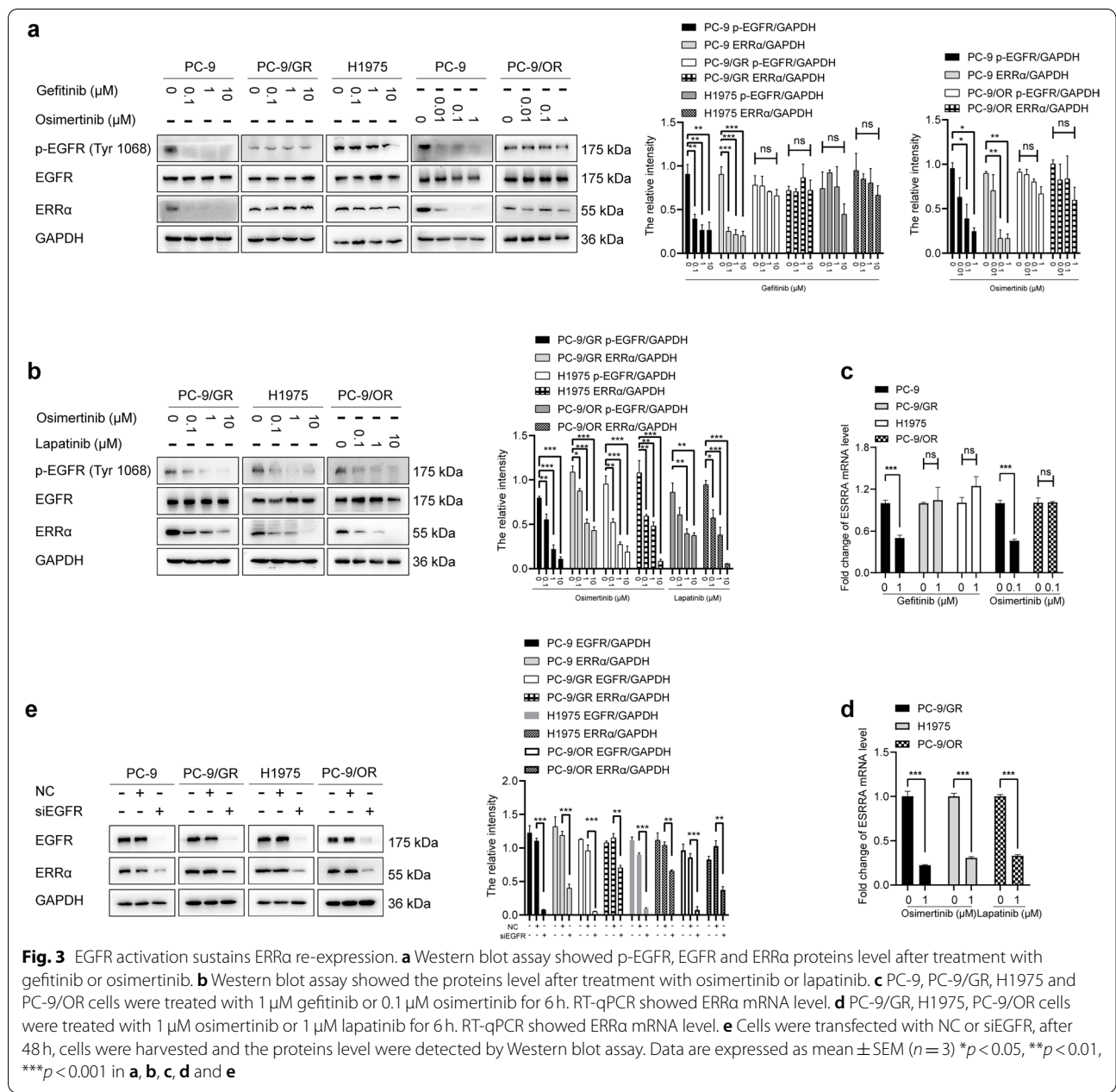


Fig. 2 Cholesterol-mediated ERRA overexpression is responsible for EGFR-TKIs resistance. **a, b** Results of RT-qPCR and Western blot assay showed ERRA mRNA and protein level in indicated cells. **c** IHC staining detected ERRA expression in tumors. **d** Cells were treated with 2.5 mM MβCD, 10 μM cholesterol or 2.5 mM MβCD + 10 μM cholesterol for 6h, then ERRA mRNA level in indicated cells was determined by RT-qPCR assay. **e** Cells were treated with 2.5 mM MβCD, 10 μM cholesterol or 2.5 mM MβCD + 10 μM cholesterol for 24h, then ERRA protein level in indicated cells was determined Western blot assay. **f** Cells were treated with gefitinib, osimertinib alone or combined with XCT790 for 48h. Then MTT assay was conducted. **g** Cells were cultured in medium with XCT790 for 48h, then fixed with cold ethanol overnight, incubated with PI/RNase staining buffer (550825, BD, Franklin Lake, NJ, USA) for 15 min. Cell cycle distribution was analyzed by flow cytometry. **h** Cells were treated with XCT790 for 48h and then incubated with DCFH-DA (S00335, Beyotime Biotechnology, Shanghai, China) for 30 min. Confocal images showed the ROS in green and the fluorescence intensity was analyzed. **i** Cells were treated with XCT790 for 48h and then fixed and incubated with 5 μM MitoSOX Red Mitochondrial Superoxide Indicator (40778E550, Yeasen, Shanghai, China) for 10 min. Confocal images showed the MitoSOX in green and the fluorescence intensity was analyzed. **j, k** Flow cytometry analysis was conducted to determine the ROS and MitoSOX accumulation in indicated cells. Data are expressed as mean ± SEM (n = 3) *p < 0.05, **p < 0.01, ***p < 0.001 in **a, b, h, i, j** and **k**. Data are expressed as mean ± SEM (n = 3) *p < 0.05, **p < 0.01, ***p < 0.001 compared to control; s p < 0.05, \$\$\$ p < 0.001 compared to MβCD in **d** and **e**



determine the statistical significance. $P < 0.05$ was considered statistically significant.

Results

Generation of gefitinib-resistant and osimertinib-resistant NSCLC cells

To generate gefitinib-resistant PC-9/GR and osimertinib-resistant PC-9/OR cells, parental PC-9 cells were exposed to increasing concentrations of gefitinib or osimertinib starting at 10 nM, until they were able to freely proliferate in 1 μM gefitinib or 500 nM osimertinib, which occurred

after 12 weeks of drug treatment (Fig. 1a, b). H1975 cells, harboring EGFR T790M mutation, were used in our study. MTT assay confirmed that cell viability of PC-9 cells was markedly inhibited by gefitinib or osimertinib compared to PC-9/GR, H1975 or PC-9/OR cells (Fig. 1c, d).

Accumulation of cholesterol promotes EGFR-TKIs resistance

Our previous studies have found that intracellular cholesterol in gefitinib-resistant NSCLC cells was higher than that in sensitive cells and was involved in gefitinib resistance [19]. However, the role of cholesterol in osimertinib

resistance and mechanisms leading to the resistance have not been fully revealed. We therefore evaluated the total cholesterol and lipid rafts cholesterol level by an Amplex[®] Red Cholesterol Assay Kit, while measured free cholesterol by filipin staining. All three types of cholesterol exhibited comparable increases in PC-9/GR, H1975, PC-9/OR cells, indicating that cholesterol accumulation occurred during NSCLC obtained gefitinib and osimertinib tolerance (Fig. 1e-g). In several studies, M β CD was used to remove cholesterol and explore the influence of cholesterol on cell viability in vitro. Our team have also done these experiments and found M β CD could sensitize NSCLC cells to EGFR-TKIs treatment. In this study, we further explored the biological function of cholesterol in the progression of gefitinib and osimertinib resistance via xenograft model. It was found that PC-9/GR, H1975, PC-9/OR xenograft tumors were larger than PC-9 xenograft counterparts both in size and weight and contained more cholesterol in tumor tissues (Fig. 1h-l). In addition, Ki67 expression was upregulated, suggesting that accumulation of cholesterol enhanced the proliferation ability of NSCLC, which might contribute to the progression of EGFR-TKIs resistance (Fig. 1m). These results revealed that accumulation of cholesterol-induced cell proliferation was responsible for both gefitinib and osimertinib resistance.

Re-expression of ERR α contributes to EGFR-TKIs resistance

To explore the underlying mechanisms of cholesterol in promoting EGFR-TKIs resistance, we determined the expression of ERR α , a nuclear receptor connected to cholesterol-mediated signal transduction [27, 35]. Firstly, we searched the OncoMine database (<https://www.oncomine.org/resource/login.html>) and found ERR α was significantly increased in lung adenocarcinoma (Fig. S1a). Kaplan-Meier survival plot showed that lower expression of ERR α resulted in a better survival (Fig. S1b). Next, the result of RT-qPCR, Western blot and IHC assays furtherly revealed that ERR α mRNA and protein level was significantly upregulated in PC-9/GR, H1975, PC-9/OR

cells and xenograft tumors compared with PC-9 cells, suggesting enhanced ERR α expression was related to NSCLC progression and development of EGFR-TKIs resistance (Fig. 2a-c). Then, we explored the relationship between changed cholesterol level and ERR α expression. It was found that M β CD decreased ERR α expression and cholesterol supplement eliminated the effect of M β CD (Fig. 2d, e). These data indicated that accumulation of cholesterol conferred NSCLC resistance to EGFR-TKIs via upregulating ERR α expression.

Subsequently, we explored the contribution of ERR α in acquired resistance to EGFR-TKIs. XCT790, an inverse agonist of ERR α , was used to downregulate the expression of ERR α . As shown, XCT790 sensitized PC-9/GR, H1975 cells to gefitinib and PC-9/OR cells to osimertinib significantly (Fig. 2f). Moreover, XCT790 induced G0/G1 phase arrest, increased total ROS and mitochondria ROS superoxide radicals in NSCLC cells (Fig. 2g-k). These data suggested that downregulation of ERR α expression sensitized resistant cells to EGFR-TKIs via increasing ROS level and causing cell cycle arrest in G0/G1 phase.

ERR α re-expression is regulated by EGFR activation

It has been reported that cholesterol influenced EGFR activation via changing the localization of EGFR on cell membrane [36]. To further investigate the signaling pathways that regulates ERR α expression during NSCLC developed drug resistance, we used EGFR-TKIs to treat NSCLC cells. It was found that gefitinib failed to decrease p-EGFR level in PC-9/GR and H1975 cells. Similarly, osimertinib failed to reduce p-EGFR level in PC-9/OR cells. However, the expression of p-EGFR was significantly depleted by gefitinib or osimertinib in sensitive PC-9 cells. Then, ERR α expression was measured under the same treatment. Notably, gefitinib or osimertinib inhibited ERR α expression in PC-9 cells. No significant changes of ERR α expression were observed in PC-9/GR, H1975, and PC-9/OR cells (Fig. 3a). To identify whether ablation of p-EGFR could then decrease ERR α expression, we reduced p-EGFR level

(See figure on next page.)

Fig. 4 Cholesterol-induced EGFR/Src/Erk signaling reactivation sustains ERR α re-expression. **a, b** Western blot and RT-qPCR assay showed ERR α expression after treatment with inhibitors of mTOR, STAT3, NF- κ B, Smad3, ROCK, EGFR, Erk or Src. **c** Cells were treated with 1 μ M gefitinib or 0.1 μ M osimertinib for 48 h, Western blot assay showed the proteins level. **d** Cells were treated with gefitinib, osimertinib, lapatinib, WH-4-023 or SCH772984 for 48 h, Western blot assay showed the proteins level. **e** Proteins in lipid rafts was extracted. Western blot assay showed EGFR and Src protein level in 20% non-lipid rafts fractions and lipid rafts fractions. **f** Cells were harvested after treatment with 10 mM M β CD for 45 min or 10 mM M β CD for 45 min + 10 μ M cholesterol for another 2 h. Proteins in lipid rafts were extracted and EGFR, Src, Caveolin1 expression was detected. **g** Co-immunoprecipitation analysis showed the EGFR and Src interaction. **h** Cells were incubated with 1 μ g/mL CTB for 1 h after treatment with M β CD or M β CD + cholesterol. Confocal images showed the lipid rafts in green and the fluorescence intensity was analyzed. **i** Immunofluorescence staining of EGFR (green) and Src (red) markers in the indicated NSCLC cells after treatment with M β CD or M β CD + cholesterol. **j** Cells were treated with M β CD or M β CD + cholesterol then subsequently with gefitinib or osimertinib for 48 h, proteins levels were detected. Data are expressed as mean \pm SEM ($n = 3$) * $p < 0.05$, ** $p < 0.01$, *** $p < 0.001$ in **a, b, c, d** and **e**. Data are expressed as mean \pm SEM ($n = 3$) ** $p < 0.01$, *** $p < 0.001$ compared to control; $^{\$}p < 0.05$, $^{\$\$}p < 0.01$, $^{\$ \$ \$}p < 0.001$ compared to M β CD in **f, g, h** and **i**. Data are expressed as mean \pm SEM ($n = 3$) * $p < 0.05$, ** $p < 0.01$, *** $p < 0.001$ compared to gefitinib or osimertinib; $^{\$}p < 0.05$, $^{\$ \$}p < 0.01$, $^{\$ \$ \$}p < 0.001$ compared to gefitinib + M β CD or osimertinib + M β CD in **j**

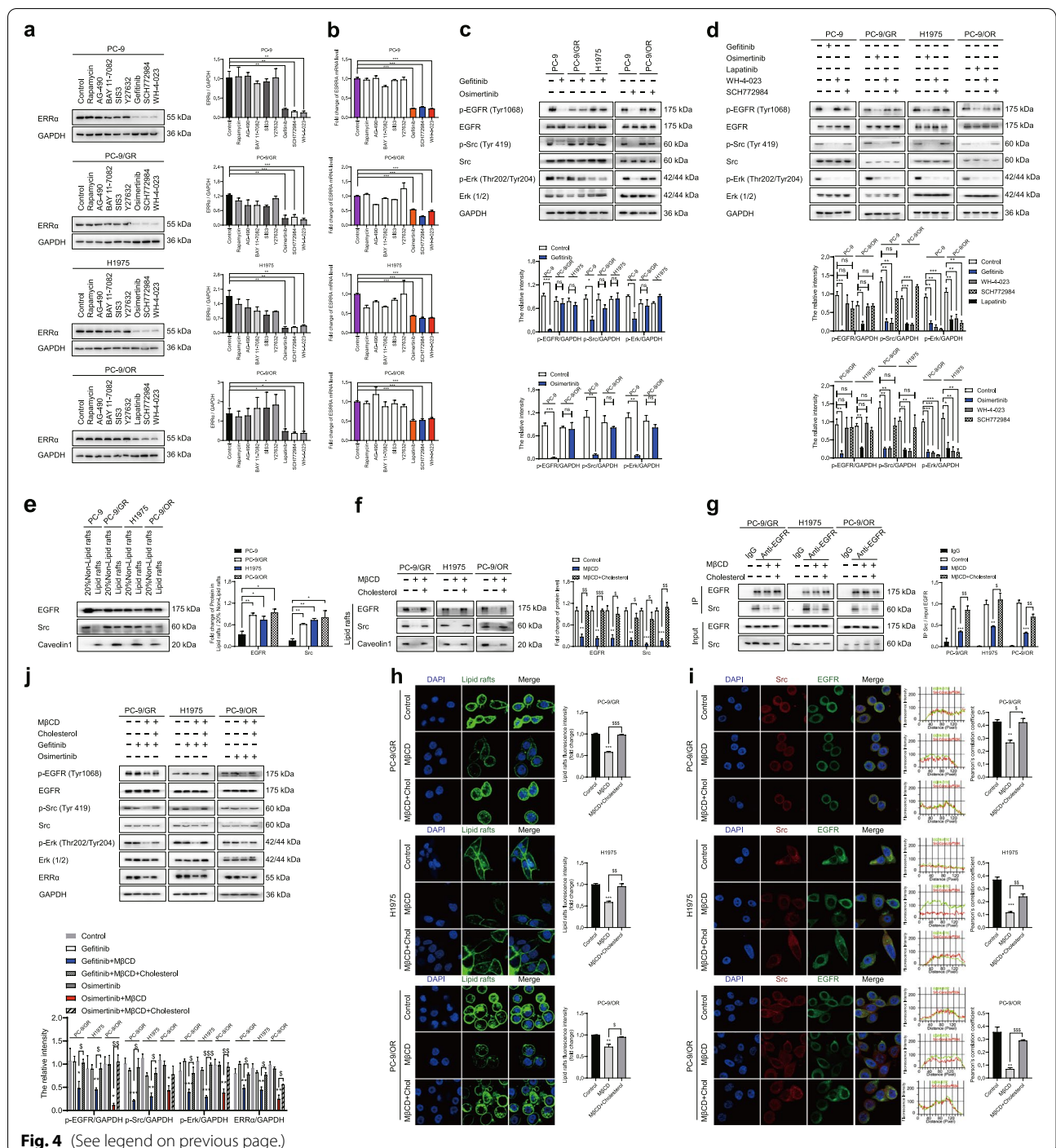


Fig. 4 (See legend on previous page.)

by osimertinib in PC-9/GR and H1975 cells, and lapatinib in PC-9/OR cells. Results showed that p-EGFR inhibition led to decreased ERRα expression (Fig. 3b). Similar consequence was observed in ERRα mRNA level (Fig. 3c, d). To rule out that the decrease of ERRα expression was caused by cell death, we treated all the four cell lines with cisplatin and noticed that cisplatin

failed to alter ERRα expression (Fig. S2a). In order to exclude the off-target effects of EGFR-TKIs, we silence EGFR by siRNA. As expected, ERRα expression was downregulated by EGFR silence in NSCLC cells (Fig. 3e). These data indicated the positive regulation of ERRα expression by EGFR signaling activation in the progress of TKIs resistance.

Cholesterol-mediated EGFR/Src/Erk signaling activation sustains ERR α re-expression

To determine which signaling pathway drives the re-expression of ERR α after EGFR signaling activation, the most commonly aberrantly activated pathways that include mTOR, STAT3, NF- κ B, Smad, ROCK, Erk and Src were tested by inhibitors rapamycin, AG-490, BAY 11-7082, SIS3, Y27632, SCH772984 and WH-4-023, respectively. We identified that the kinase inhibitors for Src and Erk consistently suppressed ERR α protein and mRNA expression in NSCLC cells (Fig. 4a, b). Further analysis showed that EGFR, Src and Erk signaling is insensitive to the inhibitory action of gefitinib or osimertinib in drug resistant cells (Fig. 4c). To dissect the regulatory hierarchy, inhibitors of EGFR, Src and Erk were used to treat NSCLC cells, respectively. As shown, p-Src and p-Erk were inhibited after EGFR signaling being blocked. In addition, WH-4-023 downregulated p-Erk expression while SCH772984 had no influence on p-Src level (Fig. 4d). These data implied that reactivation of EGFR/Src/Erk cascade sustained the re-expression of ERR α in EGFR-TKIs resistant NSCLC cells.

Next, we explored the reason by which caused EGFR/Src/Erk cascade reactivation during NSCLC resistance to EGFR-TKIs. EGFR subcellular localization is important for the activation of its downstream signaling molecules [37]. We isolated lipid rafts and non-lipid rafts fractions of NSCLC cells and found that the localization of EGFR as well as Src to lipid rafts fractions was most prominent in the EGFR-TKIs resistant cells compared to sensitive cells (Fig. 4e). When removed cholesterol by M β CD, localization of EGFR and Src to lipid rafts fractions was decreased. However, cholesterol supplement eliminated the effect of M β CD, EGFR and Src re-localized in lipid rafts (Fig. 4f). To determine whether EGFR co-localized with Src, cells were coimmunostained with EGFR and Src antibodies. It was found that co-localization between EGFR and Src occurred along the membrane of NSCLC cells. In

addition, M β CD depleted the colocalization but cholesterol restored (Fig. 4h, i). Consistently, M β CD weakened physical interaction between EGFR and Src, but cholesterol restored (Fig. 4g). Moreover, activation of EGFR/Src/Erk signaling and expression of ERR α were inhibited by gefitinib or osimertinib when M β CD was added in resistant cells. Whereas, the effect of M β CD was offset by cholesterol (Fig. 4j). These results illustrated that accumulation of cholesterol in lipid rafts during EGFR-TKIs resistance provided a platform for EGFR and Src interaction so as to activate EGFR/Src/Erk signaling pathway and finally promote ERR α expression.

The cholesterol/EGFR/Src/Erk axis downstream molecule SP1 directly promotes transcription of ERR α

Since ERR α expression was regulated by cholesterol/EGFR/Src/Erk signaling cascade, we wondered how the regulatory effect occurred. Cycloheximide (CHX) chase assay was used to evaluate the function of EGFR-TKIs on ERR α protein stability and no significant influence was observed (Fig. S2b). However, as mentioned before, blocking EGFR/Src/Erk signaling activation reduced mRNA level of ERR α . We speculated that the regulation might occur at the transcriptional level and the prediction of transcription factors was performed by UCSC Genome Browser Database (<http://genome.ucsc.edu/>). Seven potential transcription factors that regulate ERR α including CTCFL, PLAG1, CTCF, SP1, SP2, KLF16 and NRF1 were identified (Table S1). Next, we used JASPAR database (<http://jaspar.genereg.net/>) to predict transcription factor binding sites. The result demonstrated that SP1 bound to ERR α promoter region with the highest score and with the largest number of transcription factor binding sites (Tables S2, S3), which suggesting SP1 as the most possible transcription factor that regulate ERR α . In consistent with the consequence of prediction, we found that reduction of SP1 expression by plicamycin decreased ERR α expression in both mRNA and protein levels (Fig. 5a, b). The overexpression of SP1 enhanced

(See figure on next page.)

Fig. 5 SP1 transcribes ERR α directly and cholesterol/EGFR/Src/Erk axis regulates SP1 nuclear translocation. **a, b** RT-qPCR and Western blot assay showed SP1 or ERR α protein and mRNA level after treatment with SP1 inhibitor (plicamycin). **c** Cells were transfected with empty pCDNA3.1 or pCDNA3.1-SP1 for 48 h. The protein levels of SP1 and ERR α were determined by Western blot assay. **d** Cells were harvested after treatment with inhibitors of EGFR (gefitinib or osimertinib or lapatinib), Erk (SCH772984), Src (WH-4-023) for 48 h. Proteins in nucleus were extracted and SP1 expression was conducted by Western blot assay. **e** Cells were harvested after treatment with 10 mM M β CD for 45 min or 10 mM M β CD for 45 min + 10 μ M cholesterol for another 2 h, then with 1 μ M gefitinib or 0.1 μ M osimertinib for 48 h. Proteins in nucleus were extracted and SP1 expression was conducted by Western blot assay. **f** Cells were transfected with empty pCDNA3.1 or pCDNA3.1-SP1 along with inhibitors of EGFR, Erk, Src for 48 h. The protein levels of ERR α were determined by Western blot assay. **g, h** Luciferase assay was performed to determine ERR α promoter activity. **i** Binding site of SP1 was at the promoter region -1304 to -1290 bp. **j** CHIP-qPCR analysis showed that the promoter amplicons in the SP1-binding site precipitated by anti-SP1 antibody and anti-IgG antibody in H1975 cells. **k** CHIP-qPCR analysis was performed after cells treated with osimertinib, SCH772984, WH-4-023 for 48 h in H1975 cells. Data are expressed as mean \pm SEM ($n = 3$) * $p < 0.05$, ** $p < 0.01$, *** $p < 0.001$ in **a, b, c, d, g, h, j** and **k**. Data are expressed as mean \pm SEM ($n = 3$) * $p < 0.05$, ** $p < 0.01$ compared to gefitinib or osimertinib; § $p < 0.05$ compared to gefitinib + M β CD or osimertinib + M β CD in **e**. Data are expressed as mean \pm SEM ($n = 3$) * $p < 0.05$, ** $p < 0.01$, *** $p < 0.001$ compared to pCDNA3.1; § $p < 0.05$, §§ $p < 0.01$, §§§ $p < 0.001$ compared to pCDNA3.1 + inhibitors in **f**

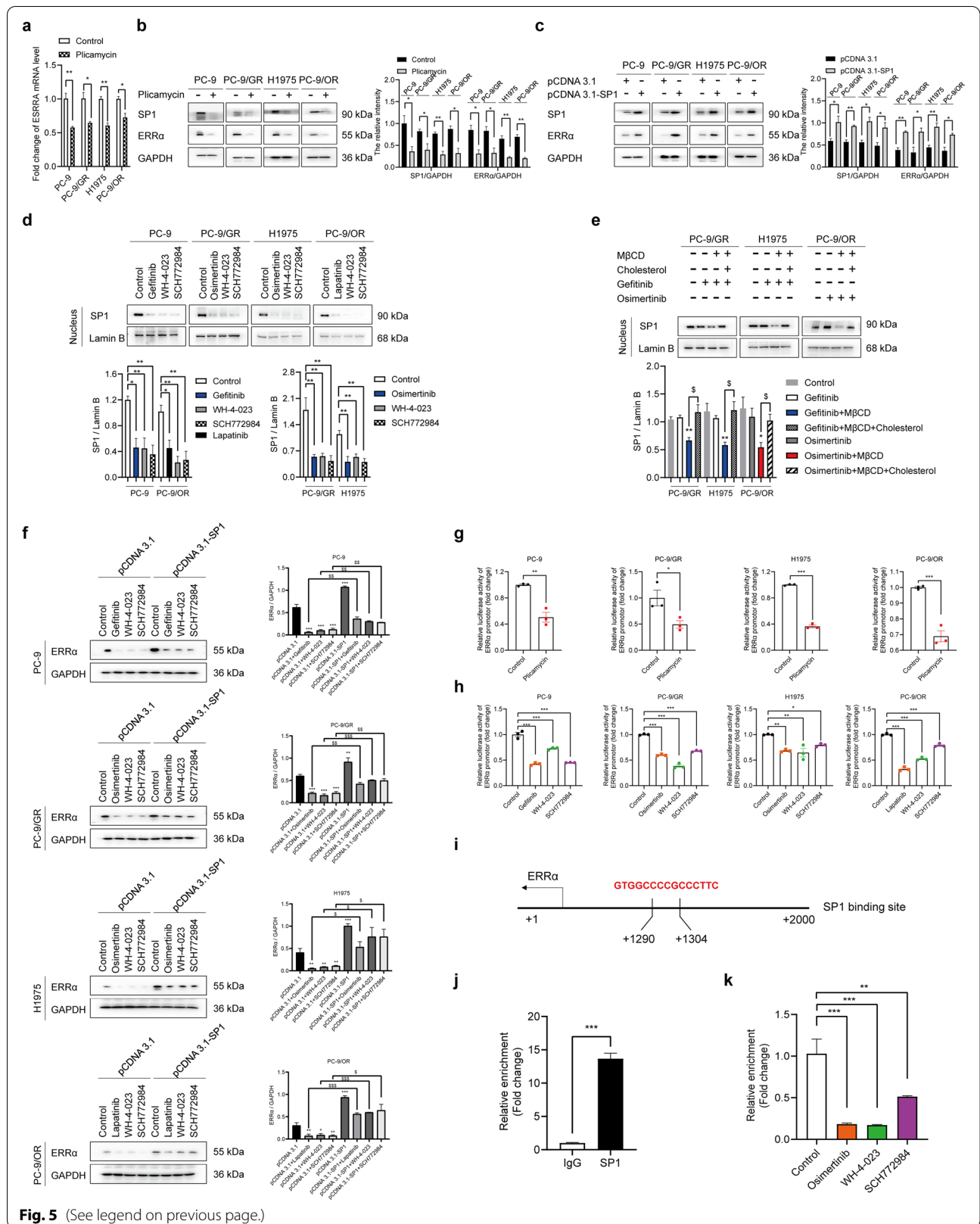


Fig. 5 (See legend on previous page.)

ERR α expression (Fig. 5c). Meanwhile, inhibitors of EGFR/Src/Erk signaling suppressed nuclear translocation of SP1 (Fig. 5d). In addition, elimination of cholesterol by M β CD treatment promoted gefitinib or osimertinib to restrain SP1 nuclear translocation. The effect was weakened by cholesterol supplement (Fig. 5e). Furthermore, overexpression of SP1 blocked the inhibitory effect of EGFR/Src/Erk inhibitors on ERR α expression (Fig. 5f).

We performed a luciferase assay and found that ERR α promoter activities were downregulated by plicamycin, gefitinib or osimertinib or lapatinib, WH-4-023 and SCH772984 in NSCLC cells (Fig. 5g, h). CHIP assay showed that compared with anti-IgG antibody, at least a 12-fold enrichment of the promoter of ERR α -binding site immunoprecipitated by anti-SP1 antibody was detected, suggesting that SP1 could directly bind to the promoter region (at -1304 to -1290 bp) of ERR α (Fig. 5i, j). Inhibition of EGFR/Src/Erk cascade could reduce the binding of SP1 and ERR α promoter (Fig. 5k). These results indicated that cholesterol-mediated EGFR/Src/Erk signaling activation could increase SP1 nuclear translocation, enabling ERR α transcription by directly binding to its promoter.

Combination of EGFR-TKIs with lovastatin or XCT790 overcome NSCLC resistance

Given the involvement of cholesterol/EGFR/Src/Erk/SP1/ERR α axis in the EGFR-TKIs resistance, we tested whether lowering cholesterol in lipid rafts and inhibiting ERR α expression could affect the sensitivity of EGFR-TKIs in NSCLC. Pharmacological lowering cholesterol using lovastatin combined with gefitinib or osimertinib lead to a significant decrease in proliferation of the drug resistant cells compared to using EGFR-TKIs alone, and the effect of lovastatin was counteracted by mevalonate or cholesterol replenishment (Fig. 6a). To investigate whether the cholesterol pathway and ERR α are functionally dependent, the drug resistant cells were treated with lovastatin and the results showed that the cells were re-sensitized to gefitinib or osimertinib, cell proliferation was suppressed and cell cycle was arrested at the G0/G1 phase. Treatment with the inverse agonist of

ERR α XCT790 exhibited similar effects. The effects of lovastatin were largely rescued by cholesterol or mevalonate addition, but this rescue was absent when ERR α expression was downregulated by XCT790, suggesting that the sensitizing effect of lovastatin on NSCLC EGFR-TKIs resistant cells are ERR α -dependent in vitro (Fig. 6b, c). The in vivo experiments confirmed that lovastatin or XCT790 synergized with gefitinib to inhibit xenograft tumor growth (Fig. 6d-j).

Discussion

Gefitinib belongs to the first-generation EGFR-TKIs and represents a major advance in the treatment of NSCLC harboring EGFR activating mutations. After treatment for about 1 year, drug resistance arises and the most frequently identified drug resistant mechanism is secondary T790M mutation of EGFR [38]. The third-generation TKI, osimertinib is designed to overcome EGFR T790M mutation and brings tremendous success as the second-line use. Osimertinib is found to be superior to gefitinib for the treatment of NSCLC patients with EGFR mutations and used as the first-line therapy in clinical trials. However, drug resistance developed inevitably. Both the first- and the third-generation EGFR-TKIs developed resistance and the mechanisms are not well understood [39]. To better understand the reason why resistance happened, we exposed human PC-9 cells to gefitinib and osimertinib for 12 weeks to establish gefitinib-resistant PC-9/GR cells and osimertinib-resistant PC-9/OR cells. H1975 cells harboring T790M mutation were also used as a gefitinib-resistant model in this study.

Cancer cells require a large amount of lipids to maintain biological membranes and sustain its characteristic of uncontrolled proliferation [40]. Cholesterol as an important component of lipids contribute to rapid cancer cell growth, metastasis and drug resistance [41]. Recently, the alteration of cholesterol homeostasis was reported in NSCLC as a result of dysregulation in cholesterol synthesis, uptake or trafficking process [17, 42]. In the present study, we found upregulated cholesterol level in both gefitinib-resistant PC-9/GR, H1975 cells and osimertinib-resistant PC-9/OR cells. The increase of cholesterol

(See figure on next page.)

Fig. 6 Lovastatin and ERR α inverse agonist enhance the sensitivity of EGFR-TKIs. **a** Cells were treated with gefitinib or osimertinib, gefitinib or osimertinib+ 10 μ M lovastatin, gefitinib or osimertinib+ 10 μ M lovastatin+ 100 μ M mevalonate, gefitinib or osimertinib+ 10 μ M lovastatin+ 10 μ M cholesterol for 48 h. Then cell viability was measured by MTT assay. **b** Cells were treated with gefitinib or osimertinib, along with lovastatin, lovastatin+ cholesterol, lovastatin+ XCT790, lovastatin+ cholesterol+ XCT790. Then cell viability was measured by MTT assay. **c** Cell cycle distribution was analyzed by flow cytometry after treatment with lovastatin, lovastatin+ MVA, lovastatin+ XCT790, lovastatin+ MVA+ XCT790. **d-j** Primary tumor gross appearance, **e** growth curves, **f** body weight, and **g** tumor weight of the PC-9/GR xenograft after treatment with indicated drugs for 21 days. **h** Cholesterol level in tumor tissue was determined. **i** Western blot assay measured ERR α protein level. **j** IHC staining detected Ki67 and ERR α expression in the indicated tumors. Data are expressed as mean \pm SEM ($n = 3$) * $p < 0.05$, ** $p < 0.01$, *** $p < 0.001$ compared to control; $^{\S}p < 0.05$, $^{\S\S}p < 0.01$, $^{\S\S\S}p < 0.001$ compared to lovastatin in **b** and **c**. Data are expressed as mean \pm SEM ($n = 3$) ** $p < 0.01$, *** $p < 0.001$ in **h** and **i**. Data are expressed as mean \pm SEM ($n = 5$) * $p < 0.05$, ** $p < 0.01$ in **g**

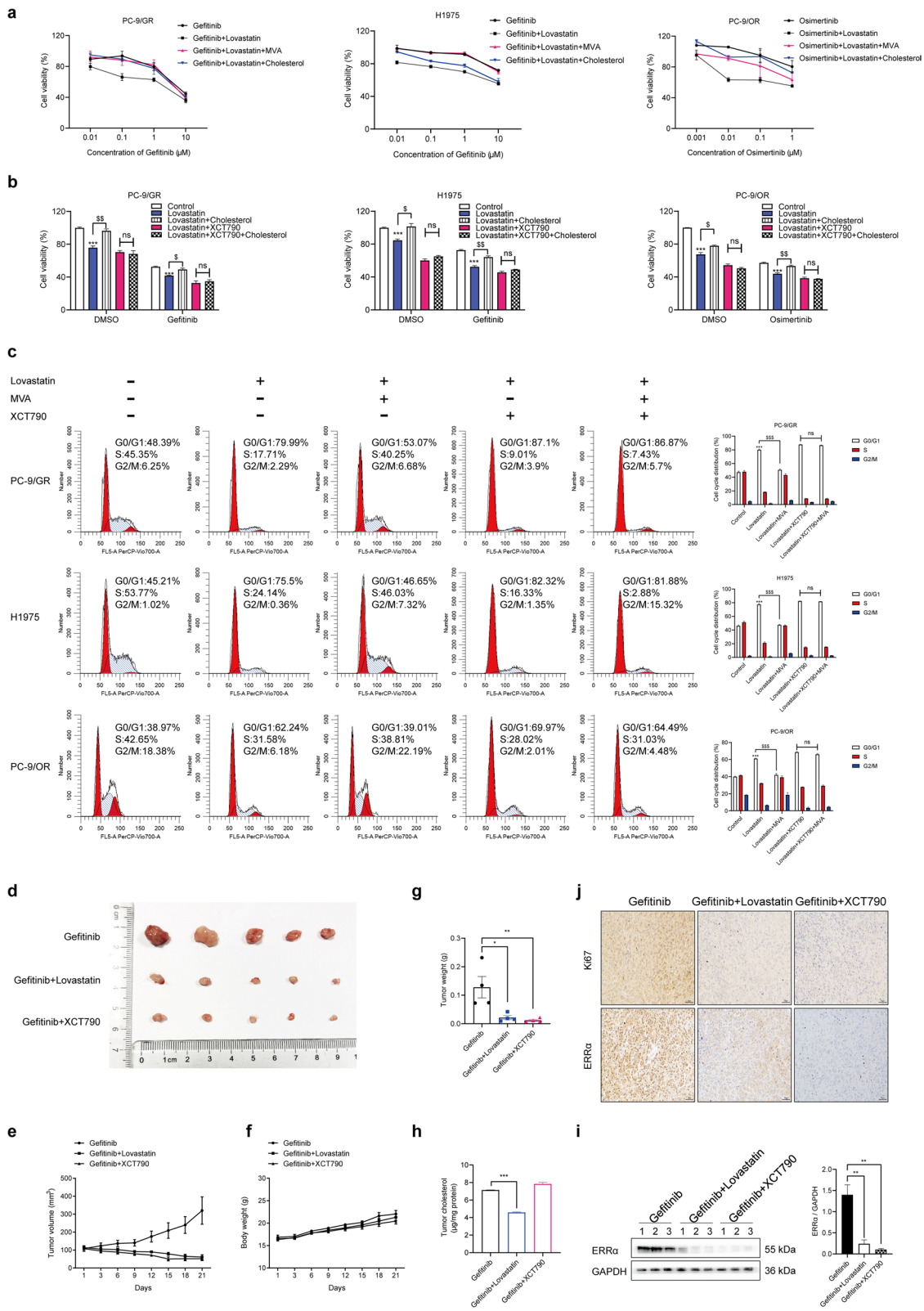
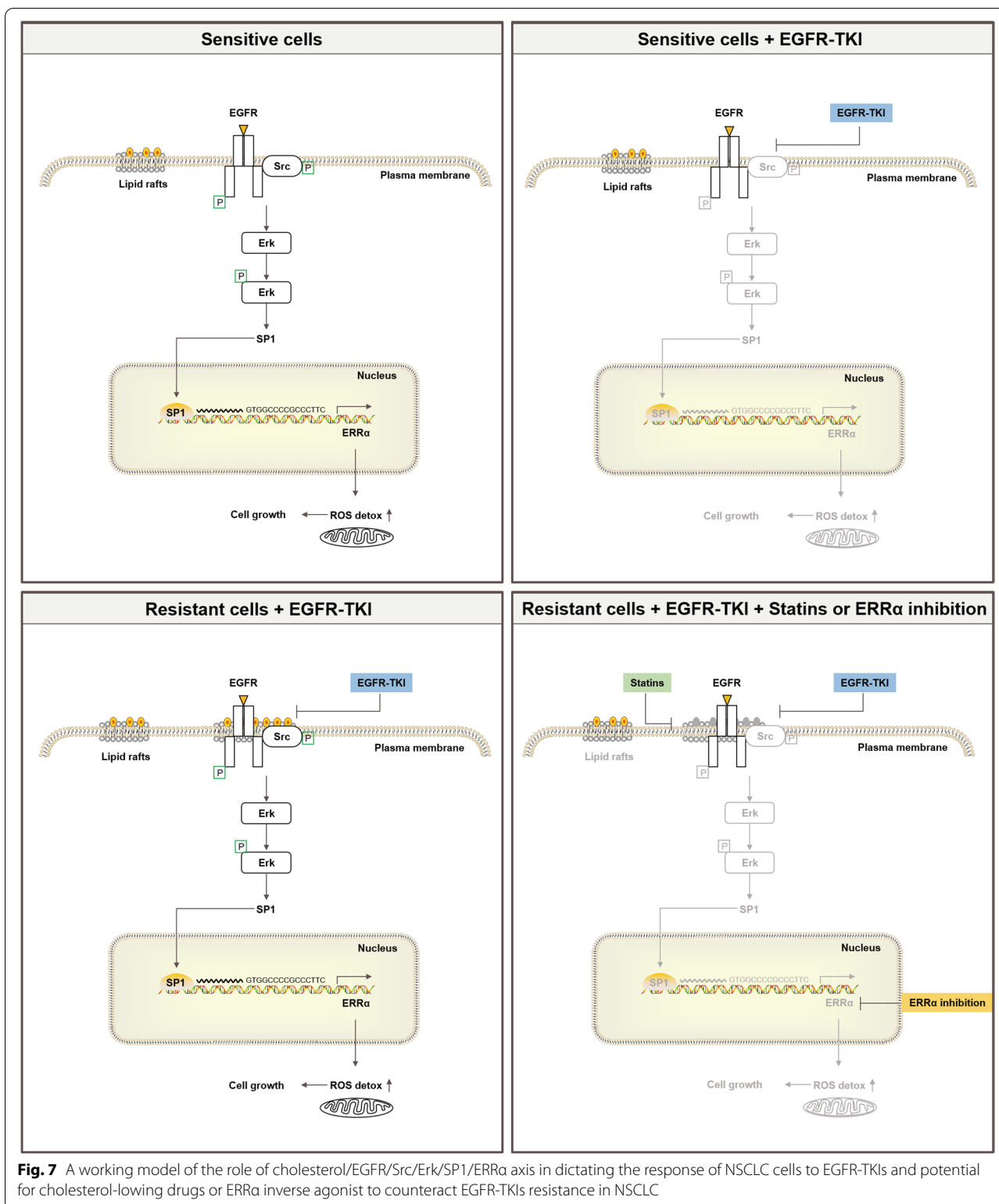


Fig. 6 (See legend on previous page.)



including intracellular total cholesterol and free cholesterol. Lipid rafts were membrane domains that enrich phospholipids, cholesterol and fatty acyl chains [43]. Pro-oncogenic proteins, such as Src, SMO and c-MET,

localize in lipid rafts and initiate signaling transduction, indicating potential involvement of lipid rafts in cancer progression [44–46]. In this work, we observed that cholesterol level in lipid rafts of resistant cells was also

increased. In xenograft tumor model, PC-9/GR, H1975, PC-9/OR showed faster growth rate and increased Ki67 expression when compared to PC-9, indicating that accumulation of cholesterol promoted growth of NSCLC.

How does cholesterol confer NSCLC cells resistant to EGFR-TKIs? We detected ERR α expression and found that compared to PC-9 cells, PC-9/GR, H1975, PC-9/OR cells showed higher mRNA and protein level of ERR α . ERR α is a nuclear transcription factor and a key regulator of energy metabolism widely expressed in organs that need a large quantity of energy [47]. Recent studies have reported that intracellular cholesterol regulated the expression and activity of ERR α in breast cancer [28, 29]. However, whether the gefitinib and osimertinib resistance promoted by cholesterol depends on ERR α is unknown. Our work revealed that cholesterol increased and M β CD decreased ERR α expression. The effect of M β CD was counteracted by cholesterol supplement. Moreover, ERR α inhibition limited the effect of cholesterol by restoring cholesterol-induced gefitinib and osimertinib resistance. Further investigation confirmed that ERR α inhibition increased the sensitivity of NSCLC cells to EGFR-TKIs through upregulating ROS level and arrested cell cycle in G0/G1 phase.

The mechanism by which cholesterol accumulation increases ERR α expression in gefitinib and osimertinib-resistant NSCLC cells is unknown. It has been reported that the activation of EGFR was linked to cholesterol level in lipid rafts [19]. The relationship between EGFR activation and ERR α expression has not been determined. Interestingly, EGFR reactivation and ERR α re-expression were observed synchronously in resistant cells under the treatment of gefitinib or osimertinib. The ERR α level was suppressed in NSCLC cells when p-EGFR expression was inhibited regardless of sensitivity to EGFR-TKIs. These data indicated the positive regulation of ERR α expression by EGFR signaling activation in the progress of TKIs resistance. Our study provided an evidence that accumulation of cholesterol recruited EGFR, Src assembly in lipid rafts and promoted interaction of the two proteins following by reactivation of EGFR/Src/Erk signaling pathway and re-expression of ERR α . Moreover, CHX chase assay showed gefitinib and osimertinib had no influence in the protein stability of ERR α . We speculated that the regulation might occur at the transcriptional level. UCSC Genome Browser Database and JASPAR database predicted SP1 as a transcription factor binding to the ERR α promoter region. SP1 is a zinc finger-type transcription factor which regulate various of genes in normal tissues and tumors [48]. Erk signaling has been reported as an upstream factor of SP1 [49]. In the current study, SP1 overexpression promoted ERR α expression and SP1 inhibition decreased ERR α expression in NSCLC cells.

Blocking of EGFR/Src/Erk signaling suppressed nuclear translocation of SP1 and overexpression of SP1 blocked the inhibitory effect of EGFR/Src/Erk inhibitors on ERR α expression. In addition, elimination of cholesterol promoted gefitinib or osimertinib to restrain SP1 nuclear translocation. However, the effect was weakened by cholesterol supplement. Our observations illustrated that SP1 was a downstream factor of cholesterol/EGFR/Src/Erk axis and regulated ERR α expression. Moreover, SP1 was identified to promote ERR α transcription directly by binding to ERR α promoter region in NSCLC. Besides, our work suggested that pharmacological lowering cholesterol by lovastatin and inhibition of ERR α represented a viable strategy to overcome EGFR-TKIs in NSCLC.

Conclusions

In conclusion, the present study uncovers a common molecular mechanism sustaining resistance to both gefitinib and osimertinib that involves the re-expression of ERR α . Long exposure to gefitinib or osimertinib lead to cholesterol of lipid rafts accumulation in NSCLC thus provided a platform for EGFR and Src interaction and re-activation of EGFR/Src/Erk signaling pathway. SP1 nuclear translocation increased and promoted ERR α transcription by binding to its promoter. Re-expression of ERR α further elicits a ROS detox context enabling cell survival despite constant exposure to EGFR-TKIs. Importantly, this study demonstrates that pharmacological lowering of cholesterol and inhibition of ERR α restore gefitinib or osimertinib sensitivity in resistant cells and xenograft tumors in vivo (Fig. 7).

Abbreviations

NSCLC: Non-small cell lung cancer; EGFR-TKIs: Epidermal growth factor receptor tyrosine kinase inhibitors; OS: Overall survival; PFS: Progression free survival; ERR α : Estrogen related receptor alpha; M β CD: Methyl- β -cyclodextrin; CHX: Cycloheximide; CHIP: Chromatin immunoprecipitation; IHC: Immunohistochemistry; RT-qPCR: Real-time quantitative polymerase chain reaction; CTB: Cholera Toxin Subunit B.

Supplementary Information

The online version contains supplementary material available at <https://doi.org/10.1186/s12943-022-01547-3>.

Additional file 1: Fig. S1. ERR α is highly expressed in NSCLC and predicts poor prognosis of NSCLC patients. **a** The expression of ERR α in normal and lung adenocarcinoma patients. The data and *P* values were obtained from the OncoMine databas. **b** Kaplan–Meier analysis of ERR α (1487_at) expression in survival of Lung cancer patients. The data and *P* values were obtained from the Kaplan–Meier Plotter database (<http://kmplot.com/analysis/index.php?p=background>).

Additional file 2: Fig. S2. Cisplatin cannot regulate ERR α expression and EGFR-TKIs fail to influence ERR α protein stability. **a** ERR α expression was measured by Western blot in NSCLC cells cultured with cisplatin (HY-17394, MCE, New Jersey, USA) for 48 h. **b** Stability of ERR α protein was measured by CHX (SC0353, Beyotime Biotechnology, Shanghai, China)

chase assay in PC-9 and H1975 cells cultured with gefitinib or osimertinib treatment. Then the ERRA protein half-life was analyzed.

Additional file 3: Table S1. Potential transcription factors were identified using the UCSC genome browser tracks in *homo sapiens* (hg38) for all profiles with a track score cutoff of 650 which equals $P < 0.000001$. **Table S2.** JASPAR database was used to predict possible transcription factor binding sites with Matrix ID, relative binding score and strand (with 90% cutoff).

Table S3. The number of predicted transcription factor binding sites in the ERRA promoter region were counted.

Acknowledgements

The study was supported by grants from the Postgraduate Innovative Project of Jiangsu Province (KYCX21_0662) to Zhenzhen Pan, Guangdong Basic and Applied Basic Research Foundation (2020A1515010605) to Jian-ye Zhang, Fund of Guangzhou Science and Technology Program (201707010048) to Jian-ye Zhang. We appreciate UniWinSci (New York) the editing service.

Authors' contributions

There are three first authors of this manuscript, and they have equally contributed to this project. Z.P. and K.W. designed the research methods, conducted the experiment, acquired and analyzed the data, prepared the manuscript. X.W. performed the experiment, reviewed and revised the manuscript. Z.J. Y.Y. and Z.X.W. provided technical and material support. Y.D. and L.H. participated in experiments. Y.Y. contributed to the language polishing of the manuscript. Furthermore, we have two corresponding authors for this manuscript. X.D. conceived and funded the projects, provided the academic interpretation of the research work, designed and revised the manuscript. J.Y.Z. funded the projects. X.D. and J.Y.Z. were also responsible for handling the revisions and resubmission of revised manuscripts. All authors read and approved the final manuscript.

Availability of data and materials

The datasets used during the current study are available from the corresponding author on reasonable request.

Declarations

Ethics approval and consent to participate

This study was approved by the Ethics Committee of China Pharmaceutical University.

Consent for publication

Not applicable.

Competing interests

The authors declare that they have no competing interests.

Author details

¹School of Basic Medicine and Clinical Pharmacy, China Pharmaceutical University, Nanjing 211198, Jiangsu, China. ²College of Pharmacy and Health Sciences, St. John's University, New York, NY 11439, USA. ³Key Laboratory of Molecular Target & Clinical Pharmacology and the State & NMPA Key Laboratory of Respiratory Disease, School of Pharmaceutical Sciences & The Fifth Affiliated Hospital, Guangzhou Medical University, Guangzhou 511436, China.

Received: 24 December 2021 Accepted: 21 February 2022

Published online: 18 March 2022

References

- Cross DA, Ashton SE, Giorghiu S, Eberlein C, Nebhan CA, Spitzler PJ, et al. AZD9291, an irreversible EGFR TKI, overcomes T790M-mediated resistance to EGFR inhibitors in lung cancer. *Cancer Discov.* 2014;4(9):1046–61.
- Kobayashi S, Boggon TJ, Dayaram T, Janne PA, Kocher O, Meyerson M, et al. EGFR mutation and resistance of non-small-cell lung cancer to gefitinib. *N Engl J Med.* 2005;352(8):786–92.
- Lynch TJ, Bell DW, Sordella R, Gurubhagavatula S, Okimoto RA, Brannigan BW, et al. Activating mutations in the epidermal growth factor receptor underlying responsiveness of non-small-cell lung cancer to gefitinib. *N Engl J Med.* 2004;350(21):2129–39.
- Mok TS, Wu YL, Ahn MJ, Garassino MC, Kim HR, Ramalingam SS, et al. Osimertinib or platinum-Pemetrexed in EGFR T790M-positive lung Cancer. *N Engl J Med.* 2017;376(7):629–40.
- Mok TS, Wu YL, Thongprasert S, Yang CH, Chu DT, Saijo N, et al. Gefitinib or carboplatin-paclitaxel in pulmonary adenocarcinoma. *N Engl J Med.* 2009;361(10):947–57.
- Paez JG, Janne PA, Lee JC, Tracy S, Greulich H, Gabriel S, et al. EGFR mutations in lung cancer: correlation with clinical response to gefitinib therapy. *Science.* 2004;304(5676):1497–500.
- Rosell R, Carcereny E, Gervais R, Vergnenegre A, Massuti B, Felip E, et al. Erlotinib versus standard chemotherapy as first-line treatment for European patients with advanced EGFR mutation-positive non-small-cell lung cancer (EURTAC): a multicentre, open-label, randomised phase 3 trial. *Lancet Oncol.* 2012;13(3):239–46.
- Schmid S, Li JJN, Leighl NB. Mechanisms of osimertinib resistance and emerging treatment options. *Lung Cancer.* 2020;147:123–9.
- Skoulidis F, Heymach JV. Co-occurring genomic alterations in non-small-cell lung cancer biology and therapy. *Nat Rev Cancer.* 2019;19(9):495–509.
- Soria JC, Ohe Y, Vansteenkiste J, Reungwetwattana T, Chewaskulyong B, Lee KH, et al. Osimertinib in untreated EGFR-mutated advanced non-small-cell lung cancer. *N Engl J Med.* 2018;378(2):113–25.
- Zhang Z, Guo X, To KKW, Chen Z, Fang X, Luo M, et al. Olmutinib (HM61713) reversed multidrug resistance by inhibiting the activity of ATP-binding cassette subfamily G member 2 in vitro and in vivo. *Acta Pharm Sin B.* 2018;8(4):563–74.
- Hirsch HA, Iliopoulos D, Joshi A, Zhang Y, Jaeger SA, Buluyk M, et al. A transcriptional signature and common gene networks link cancer with lipid metabolism and diverse human diseases. *Cancer Cell.* 2010;17(4):348–61.
- Cheng C, Geng F, Cheng X, Guo D. Lipid metabolism reprogramming and its potential targets in cancer. *Cancer Commun (Lond).* 2018;38(1):27.
- Kuzu OF, Noory MA, Robertson GP. The role of cholesterol in Cancer. *Cancer Res.* 2016;76(8):2063–70.
- Lingwood D, Simons K. Lipid rafts as a membrane-organizing principle. *Science.* 2010;327(5961):46–50.
- Giacomini I, Gianfanti F, Desbats MA, Orso G, Berretta M, Prayer-Galetti T, et al. Cholesterol metabolic reprogramming in Cancer and its pharmacological modulation as therapeutic strategy. *Front Oncol.* 2021;11:682911.
- Luo Y, Yang Y, Peng P, Zhan J, Wang Z, Zhu Z, et al. Cholesterol synthesis disruption combined with a molecule-targeted drug is a promising metabolic therapy for EGFR mutant non-small cell lung cancer. *Transl Lung Cancer Res.* 2021;10(1):128–42.
- Ali A, Levantini E, Fhu CW, Teo JT, Clohessy JG, Goggi JL, et al. CAV1 - GLUT3 signaling is important for cellular energy and can be targeted by atorvastatin in non-small cell lung Cancer. *Theranostics.* 2019;9(21):6157–74.
- Chen Q, Pan Z, Zhao M, Wang Q, Qiao C, Miao L, et al. High cholesterol in lipid rafts reduces the sensitivity to EGFR-TKI therapy in non-small cell lung cancer. *J Cell Physiol.* 2018;233(9):6722–32.
- Deblois G, St-Pierre J, Giguere V. The PGC-1/ERR signaling axis in cancer. *Oncogene.* 2013;32(30):3483–90.
- Wang J, Wang Y, Wong C. Oestrogen-related receptor alpha inverse agonist XCT-790 arrests A549 lung cancer cell population growth by inducing mitochondrial reactive oxygen species production. *Cell Prolif.* 2010;43(2):103–13.
- Vernier M, McGuiRK S, Dufour CR, Wan L, Audet-Walsh E, St-Pierre J, et al. Inhibition of DNMT1 and ERRalpha crosstalk suppresses breast cancer via derepression of IRF4. *Oncogene.* 2020;39(41):6406–20.
- Zhou S, Xia H, Xu H, Tang Q, Nie Y, Gong QY, et al. ERRalpha suppression enhances the cytotoxicity of the MEK inhibitor trametinib against colon cancer cells. *J Exp Clin Cancer Res.* 2018;37(1):218.
- Huang JW, Guan BZ, Yin LH, Liu LH, Hu B, Zheng QY, et al. Effects of estrogen-related receptor alpha (ERRalpha) on proliferation and metastasis of human lung cancer A549 cells. *J Huazhong Univ Sci Technolog Med Sci.* 2014;34(6):875–81.
- Zhang J, Guan X, Liang N, Li S. Estrogen-related receptor alpha triggers the proliferation and migration of human non-small cell lung cancer via interleukin-6. *Cell Biochem Funct.* 2018;36(5):255–62.

26. Li P, Wang J, Wu D, Ren X, Wu W, Zuo R, et al. ERRalpha is an aggressive factor in lung adenocarcinoma indicating poor prognostic outcomes. *Cancer Manag Res.* 2019;11:8111–23.
27. Ghanbari F, Mader S, Philip A. Cholesterol as an Endogenous Ligand of ERRalpha Promotes ERRalpha-Mediated Cellular Proliferation and Metabolic Target Gene Expression in Breast Cancer Cells. *Cells.* 2020;9(8):1765.
28. Brindisi M, Fiorillo M, Frattaruolo L, Sotgia F, Lisanti MP, Cappello AR. Cholesterol and Mevalonate: Two Metabolites Involved in Breast Cancer Progression and Drug Resistance through the ERRalpha Pathway. *Cells.* 2020;9(8):1819.
29. Ghanbari F, Fortier AM, Park M, Philip A. Cholesterol-Induced Metabolic Reprogramming in Breast Cancer Cells Is Mediated via the ERRalpha Pathway. *Cancers (Basel).* 2021;13(11):2605.
30. Fujimoto J, Nakagawa Y, Toyoki H, Sakaguchi H, Sato E, Tamaya T. Estrogen-related receptor expression in placenta throughout gestation. *J Steroid Biochem Mol Biol.* 2005;94(1-3):67–9.
31. Jung HK, Kim S, Park RW, Park JY, Kim IS, Lee B. Bladder tumor-targeted delivery of pro-apoptotic peptide for cancer therapy. *J Control Release.* 2016;235:259–67.
32. Dunn KW, Kamocka MM, McDonald JH. A practical guide to evaluating colocalization in biological microscopy. *Am J Physiol Cell Physiol.* 2011;300(4):C723–42.
33. Anguisola S, McCormack WJ, Morrin MA, Higgins WJ, Fox DM, Worrall DM. Pigment epithelium-derived factor (PEDF) interacts with transportin SR2, and active nuclear import is facilitated by a novel nuclear localization motif. *PLoS One.* 2011;6(10):e26234.
34. Fang CH, Lin YT, Liang CM, Liang SM. A novel c-kit/phospho-prohibitin axis enhances ovarian cancer stemness and chemoresistance via Notch3-PBX1 and beta-catenin-ABCG2 signaling. *J Biomed Sci.* 2020;27(1):42.
35. Wei W, Schwaid AG, Wang X, Wang X, Chen S, Chu Q, et al. Ligand activation of ERRalpha by cholesterol mediates statin and bisphosphonate effects. *Cell Metab.* 2016;23(3):479–91.
36. Balbis A, Posner BL. Compartmentalization of EGFR in cellular membranes: role of membrane rafts. *J Cell Biochem.* 2010;109(6):1103–8.
37. Irwin ME, Bohin N, Boerner JL. Src family kinases mediate epidermal growth factor receptor signaling from lipid rafts in breast cancer cells. *Cancer Biol Ther.* 2011;12(8):718–26.
38. Camidge DR, Pao W, Sequist LV. Acquired resistance to TKIs in solid tumours: learning from lung cancer. *Nat Rev Clin Oncol.* 2014;11(8):473–81.
39. Scalvini L, Castelli R, La Monica S, Tiseo M, Alfieri R. Fighting tertiary mutations in EGFR-driven lung-cancers: current advances and future perspectives in medicinal chemistry. *Biochem Pharmacol.* 2021;190:114643.
40. Cao Y. Adipocyte and lipid metabolism in cancer drug resistance. *J Clin Invest.* 2019;129(8):3006–17.
41. Xu H, Zhou S, Tang Q, Xia H, Bi F. Cholesterol metabolism: new functions and therapeutic approaches in cancer. *Biochim Biophys Acta Rev Cancer.* 1874;2020(1):188394.
42. Kim H, Choi SY, Lim J, Lindroth AM, Park YJ. EHMT2 Inhibition Induces Cell Death in Human Non-Small Cell Lung Cancer by Altering the Cholesterol Biosynthesis Pathway. *Int J Mol Sci.* 2020;21(3):1002.
43. Sezgin E, Levental I, Mayor S, Eggeling C. The mystery of membrane organization: composition, regulation and roles of lipid rafts. *Nat Rev Mol Cell Biol.* 2017;18(6):361–74.
44. Zeng J, Zhang H, Tan Y, Sun C, Liang Y, Yu J, et al. Aggregation of lipid rafts activates c-met and c-Src in non-small cell lung cancer cells. *BMC Cancer.* 2018;18(1):611.
45. Shi D, Lv X, Zhang Z, Yang X, Zhou Z, Zhang L, et al. Smoothed oligomerization/higher order clustering in lipid rafts is essential for high hedgehog activity transduction. *J Biol Chem.* 2013;288(18):12605–14.
46. Irwin ME, Mueller KL, Bohin N, Ge Y, Boerner JL. Lipid raft localization of EGFR alters the response of cancer cells to the EGFR tyrosine kinase inhibitor gefitinib. *J Cell Physiol.* 2011;226(9):2316–28.
47. Luo J, Sladek R, Carrier J, Bader JA, Richard D, Giguere V. Reduced fat mass in mice lacking orphan nuclear receptor estrogen-related receptor alpha. *Mol Cell Biol.* 2003;23(22):7947–56.
48. Jiang NY, Woda BA, Banner BF, Whalen GF, Dresser KA, Lu D. Sp1, a new biomarker that identifies a subset of aggressive pancreatic ductal adenocarcinoma. *Cancer Epidemiol Biomark Prev.* 2008;17(7):1648–52.
49. Zhang Y, Chen HX, Zhou SY, Wang SX, Zheng K, Xu DD, et al. Sp1 and c-Myc modulate drug resistance of leukemia stem cells by regulating survivin expression through the ERK-MSK MAPK signaling pathway. *Mol Cancer.* 2015;14:56.

Publisher's Note

Springer Nature remains neutral with regard to jurisdictional claims in published maps and institutional affiliations.

Ready to submit your research? Choose BMC and benefit from:

- fast, convenient online submission
- thorough peer review by experienced researchers in your field
- rapid publication on acceptance
- support for research data, including large and complex data types
- gold Open Access which fosters wider collaboration and increased citations
- maximum visibility for your research: over 100M website views per year

At BMC, research is always in progress.

Learn more biomedcentral.com/submissions

